Hindawi Publishing Corporation
Physics Research International
Volume 2012, Article ID 172987, 8 pages
doi:10.1155/2012/172987

Review Article

Nuclear Wavepacket Dynamics of Alkali Adsorbates on Metal Surfaces Studied by Time-Resolved Second Harmonic Generation

Kazuya Watanabe and Yoshiyasu Matsumoto

Department of Chemistry, Graduate School of Science, Kyoto University, Kyoto 606-8502, Japan

Correspondence should be addressed to Kazuya Watanabe, kw@kuchem.kyoto-u.ac.jp

Received 2 December 2011; Accepted 15 February 2012

Academic Editor: Goro Mizutani

This paper reviews recent efforts to understand the dynamics of coherent surface vibrations of alkali atoms adsorbed on metal surfaces. Time-resolved second harmonic generation is used for the coherent excitation and detection of the nuclear wavepacket dynamics of the surface modes. The principles of the measurement and the experimental details are described. The main focus is on coverage and excitation photon energy dependences of the coherent phonon dynamics for Na-, K-, and Cs-covered Cu(111). The excitation mechanism of the coherent phonon has been revealed by the ultrafast time-domain technique and theoretical modelings.

1. Introduction

When a material is excited with a laser pulse with duration shorter than a vibrational period, coherent vibration in which molecules or atoms oscillate in phase over a macroscopic region is induced [1, 2]. This "impulsive" excitation of vibrational (nuclear) wavepacket has been observed for a variety of substances: from gas-phase molecules to solids. The coherent nuclear motions can be probed via modulation of optical response of the materials due to the influence of the nuclear displacement on the complex refractive indices. Typically, changes of absorbance or reflectance of a time-delayed probe pulse are measured as a function of pump-probe delay time and the coherent vibrational motions emerge as oscillatory intensity modulations. Elucidation of the excitation mechanism and the decay dynamics of the nuclear wavepacket leads to detailed understanding of the electron-vibration (phonon) coupling and photochemical dynamics.

Phenomenological equation of motion of the amplitude $Q(t)$ of the relevant coherent vibrational mode can be described as a forced harmonic oscillator with damping,

$$\ddot{Q}(t) + 2\beta\dot{Q}(t) + \Omega_0^2 Q(t) = \frac{F(t)}{\mu}, \tag{1}$$

where $\Omega_0/2\pi$ is the natural frequency of the undamped oscillator, β is the damping rate, μ is the effective mass of the oscillator, and $F(t)$ is the force exerted on the system. With this driving force, a time evolution of the amplitude is given by [3]

$$Q(t) \propto \cos(\Omega_1 t - \phi)e^{-\beta t}, \tag{2}$$

where $\Omega_1 = \sqrt{\Omega_0^2 - \beta^2}$ and ϕ is the initial phase. The initial phase provides information on the nature of the driving force through the following general relationship [3]:

$$\tan\phi = \frac{\mathrm{Im}\left[i\widetilde{F}(-\Omega_1 - i\beta)\right]}{\mathrm{Re}\left[i\widetilde{F}(-\Omega_1 - i\beta)\right]}, \tag{3}$$

where $\widetilde{F}(\Omega)$ is the Fourier transform of $F(t)$. If the driving force is impulsive, the initial phase is $\pi/2$ and the oscillation becomes sin-like. If the force is a step function like in time domain, the initial phase is 0 or π and the oscillation becomes cos-like.

While there exists a body of literature on coherent vibration in gas phase and in bulk condensed matter, those at surfaces or interfaces are relatively less explored. This is because the signal intensity from surface monolayer of atoms

and molecules is generally very small and the experimental observation is demanding. Second-order nonlinear optical process paves the way for probing the dynamics at surfaces and interfaces. We have found that time-resolved second harmonic generation (TRSHG) [4] is a powerful technique to probe the coherent vibration (phonon) of alkali atoms adsorbed on metal surfaces [5–8]. In this paper, we describe our recent achievements in understanding the dynamics of coherent surface phonons at alkali-metal-covered metal surfaces [9–11]. One of the most important issues in the study of coherent phonons at metal surfaces is to determine what electronic transition is most responsible for their creation. Thus, we focus on the electronic structure of alkali-covered metal surfaces and the excitation mechanism of the coherent vibration.

2. Alkali Metals on Metal Surfaces and Enhancement of Nonlinear Susceptibility

Here we describe general features of alkali atoms on metal surfaces particularly focusing on their electronic structure and optical responses. Overlayers of alkali metal atoms on metal surfaces are typical model systems of metals on metals, and detailed information on the adsorption geometries [12], the vibrational [13, 14] and electronic structures [15], and the electronic excitation [16] has been reported. Here we briefly summarize some features of the electronic structure of alkali-covered Cu(111) [17]. The bonding of alkali atoms on metal surfaces strongly depends on alkali coverage. At low coverages the work function decreases sharply with the increase of the coverage. As the coverage increases further, the work function reaches to a minimum and increases toward that of the bulk alkali metal. In the classical model of Gurney [18], an alkali atom donates an outermost occupied *s* electron to the metal to form a positive ion at the low coverages; this results in a surface dipole layer that induces the large drop in work function. As the coverage increases, the lateral interaction of alkali atoms becomes stronger; alkali atoms are depolarized and the alkali overlayer becomes metallic.

The metallic character of the alkali overlayer at high coverages is due to emergence of two bands: an overlayer resonance (OR) located below the *L*-band gap and a quantum well state (QWS) around the Fermi level. These bands correlate to those of a free standing alkali monolayer in the vacuum: the *s*-like lowest and the p_z-like second lowest bands [19]. When the monolayer is brought closer to the metal surface, these bands are stabilized by the interaction with the metal, while maintaining the integrity. The *s*-like band correlates to OR; the p_z-like band correlates to QWS. Because QWS is located in the *L*-band gap, its wave function is localized at the surface. In contrast, the wave function of OR extends more into the substrate, because it is located below the lower edge of *L*-band gap.

It has been known that alkali overlayers enhance the conversion efficiency of second harmonic generation (SHG) by a few orders of magnitude in comparison with clean metal surfaces [20]. When an optical field $\vec{E}$ increases, the macroscopic polarization induced in a medium $\vec{P}$ shows nonlinearity with respect to the field. The nonlinear polarization responsible for SHG is given by

$$\vec{P}^{(2)}(2\omega) = \chi^{(2)}(2\omega, \omega, \omega) : \vec{E}(\omega)\vec{E}(\omega), \tag{4}$$

where $\chi^{(2)}(2\omega, \omega, \omega)$ is the second-order nonlinear susceptibility for SHG. In a medium with centrosymmetry, $\chi^{(2)}$ of the medium is zero within the electric dipole approximation. In contrast, at a surface where centrosymmetry is generally broken, dipole-allowed SH signals are generated from the surface. Thus, SH generation spectroscopy provides an inherent surface sensitivity if bulk materials have centrosymmetry [21].

Figure 1 shows how the SH intensity of 800 nm ($h\nu = 1.55$ eV) photons depends on coverage of alkali atoms on Cu(111) surfaces. The coverage has been calibrated by measuring the ratio of Auger electron signals of alkali adsorbates to that of the substrates as a function of the deposition time [10]. Throughout this paper, we define the alkali coverage as one monolayer when the first layer is completed, although in the original articles the coverage was defined as a ratio of the alkali atomic density to that of the substrate.

The SH intensity is enhanced by a few orders of magnitude compared to the clean surface when alkali atoms are adsorbed [10]. There are two major origins of the SH enhancement associated with alkali adsorption: interband transitions between surface electronic states and multipole plasmon excitation [16, 22]. At the low coverages, interband transitions from occupied surface state (SS) to alkali-induced antibonding state (AS) [23] or from SS to image potential states (IPSs) become resonant to $2h\nu$ ($= 3.10$ eV) below $\theta = 0.4$. Therefore, the "resonant" peaks observed at $\theta \leq 0.5$ in Figure 1 are likely due to resonant or near-resonant transitions in which the surface localized bands, SS, AS, and IPSs, are involved. As coverage increases over $\theta = 0.4$, the alkali overlayer is depolarized and the metallic QWS and OR bands are formed. The transitions from the occupied-OR band to the *s, p* bands of the substrate and interband transitions from QWS to the substrate bands contribute to the SH intensity.

At $\theta \sim 1.0$, the contribution to SH intensity from multipole plasmon excitation may be larger than that from the interband transitions because the photon energy $2h\nu$ ($= 3.1$ eV) is close to plasmon resonance energies: $\hbar\omega_p = 3.8$ and 3.5 eV for K and Cs, respectively, where $\hbar\omega_p$ is the bulk-plasma frequency. Irradiation of a metal surface with an oscillating electromagnetic field induces a dynamic screening field [24]. If the optical frequency is close to $0.8\,\omega_p$, electronic transitions at the surface excite resonantly a damped collective mode along the surface normal. This coupling between the optical field and multipole plasmons at the surface results in the local field enhancement of the nonlinear response such as SHG. Liebsch calculated the frequency dependence of SH dipole moments of alkali overlayers at $\theta = 1$ by using the time-dependent density-functional method [22] and found that the resonant peak of the imaginary part of the dipole moment is located at 2.0,

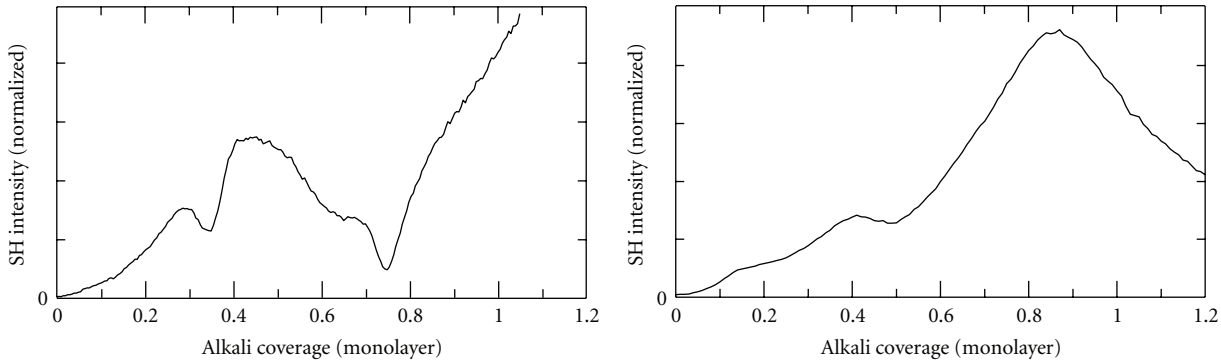

Figure 1: Second harmonic intensity as a function of coverage of (a) potassium and (b) cesium on Cu(111) surface. The excitation wavelength is 800 nm (1.55 eV). Note that here one monolayer corresponds to the saturation coverage of the first layer, although in the original papers one monolayer has been defined as the atomic densities of the substrates.

1.4, and 1.3 eV for Na, K, and Cs on Al, respectively. The photon energy of $h\nu = 1.55$ eV is close to the resonance of the potassium overlayer at $\theta = 1$. This is consistent with the significant increase of SH intensity at the saturation coverage of K on Cu(111) as shown in Figure 1.

3. Principles of the Time-Resolved Second Harmonic Generation

In TRSHG spectroscopy, the SH intensity of a probe pulse is measured as a function of pump-probe delay time t. Transient changes in the SH intensity $\Delta I_{\mathrm{SH}}(t)$ are defined as

$$\Delta I_{\mathrm{SH}}(t) = \frac{\left[I_{\mathrm{SH}}(\mathrm{t}) - I^0_{\mathrm{SH}}\right]}{I^0_{\mathrm{SH}}}, \tag{5}$$

where $I_{\mathrm{SH}}(t)$ is the SH intensity at a delay time t and I^0_{SH} is that without a pump pulse, respectively.

When a metallic alkali monolayer is brought from the vacuum to a metal surface, the electronic bands of the free-standing alkali monolayer shift their binding energies as a result of interactions with the metal substrate. Thus, the binding energies of the alkali-induced bands depend on the displacement of the overlayer along the surface normal δQ. Consequently, the oscillation of δQ due to coherent excitation of the alkali-substrate stretching mode (S mode) alters the binding energies and populations of the alkali-induced bands; in this way, the coherent vibration of alkali atoms contributes to TRSHG signals. Because the lateral displacements of the alkali overlayer are not expected to shift the binding energies of alkali-induced bands as large as the vertical ones, the lateral motions of alkali adsorbates contribute little to TRSHG signals.

The modulation of $\chi^{(2)}$ due to the displacement of the ith phonon mode, δQ_i, can be approximated by (neglecting the modulation due to the electronic population change) [25]

$$\chi^{(2)} = \chi^{(2)}|_0 + \sum_i \left(\frac{\partial \chi^{(2)}}{\partial Q_i}\right)_0 \delta Q_i. \tag{6}$$

Because the SH intensity is proportional to the square of $|\chi^{(2)}|$, the dominant contribution of the coherent phonons to $\Delta I_{\mathrm{SH}}(t)$ is expressed as

$$\Delta I_{\mathrm{SH}}(t) \propto \chi^{(2)}|_0 \cdot \sum_i \left(\frac{\partial \chi^{(2)}}{\partial Q_i}\right)_0 \delta Q_i, \tag{7}$$

in which the SH intensity modulation is proportional to the displacement of the phonon mode.

4. TRSHG Experimental Setup [7, 10, 11]

The experiments were carried out in an ultrahigh vacuum chamber equipped with a cylindrical analyzer for Auger electron spectroscopy (AES) and low energy electron diffraction. Alkali atoms from a degassed alkali dispenser (SAES Getters) were deposited on a clean substrate at 90–110 K. The coverage was determined by the ratio of AES intensity of adsorbate and substrate atoms.

For the TRSHG measurements we used home-made non-collinear optical parametric amplifiers (NOPAs) pumped with the second harmonic (400 nm) output of a Ti: sapphire regenerative amplifier (1 kHz, 130 fs). NOPA delivers 25–35 fs pulses whose center photon energy is tunable from 2.0 eV to 2.4 eV. In addition, we also used a fundamental (800 nm) output of the regenerative amplifier with an extra pulse compression apparatus: the output was focused into a 2 m long cylindrical tube filled with Kr gas. The bandwidth of the output pulse is broadened and the pulse compression to 35 fs was attained with additional multiple reflections on negative group-delay dispersion mirrors.

p-Polarized pump and probe pulses were focused onto the sample with an incidence angle of about 70 degrees, and the second harmonic intensity of the probe pulse that is generated coaxially with the probe was detected as a function of pump-probe delay. All the measurements were carried out with sample temperature at 85–110 K.

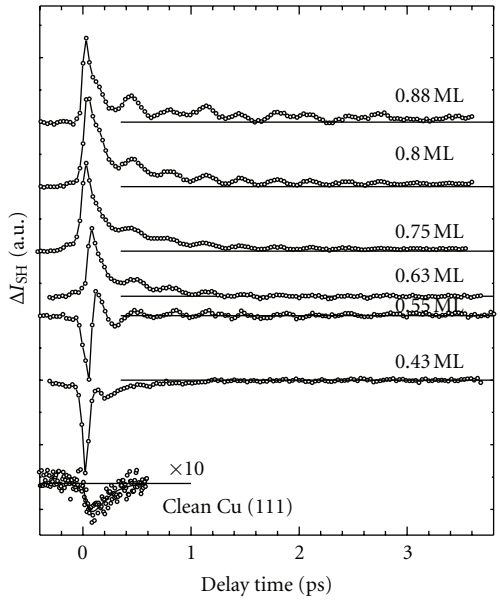

Figure 2: Coverage dependence of TRSHG traces for K/Cu(111). Potassium coverages are indicated. 1 ML corresponds to the saturation coverage of the first layer [10]. The pump pulse photon energy was 2.20 eV, and probe pulse photon energy was 1.55 eV.

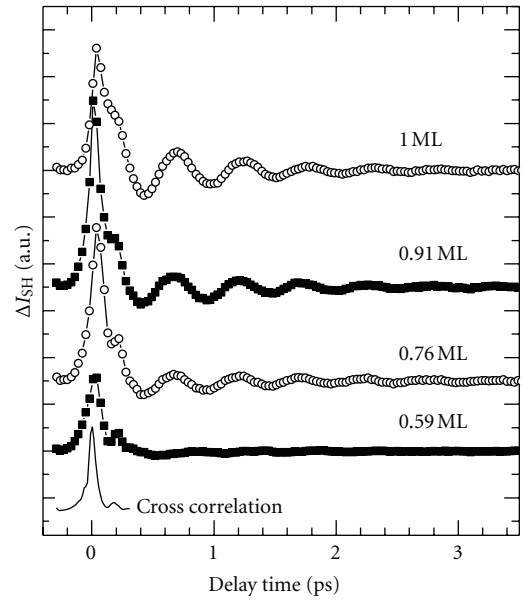

Figure 3: Coverage dependence of TRSHG traces for Cs/Cu(111). Cesium coverages are indicated. 1 ML corresponds to the saturation coverage of the first layer. The bottom trace is a cross-correlation curve between pump and probe. The pump pulse photon energy was 1.55 eV, while the probe pulse photon energy was 2.20 eV.

5. Coverage Dependence

Figures 2 and 3 show coverage dependence of TRSHG traces from K and Cs on Cu(111). In both cases, the coherent nuclear motions emerge as damped oscillatory components. The TRSHG traces are analyzed by using singular value decomposition [7] assuming the following linear combination of damped cosinusoids and exponential decay components:

$$\Delta I_{\mathrm{SH}} = \sum_i A_i \exp\left(\frac{-t}{\tau_i}\right) \cos(\omega_i t + \phi_i) + \sum_i B_i \exp\left(\frac{-t}{\tau_i}\right), \tag{8}$$

where ω_i and ϕ_i are phonon frequency and initial phase, respectively, and τ_i is a dephasing time of a vibrational coherence or a decay time of a background component. The first term represents the coherent nuclear motions of the S modes and the second term describes the SH modulation due to the electronic population changes.

The oscillation frequencies were found to be 3.0-3.1 THz (at $\theta < 0.8$) for K/Cu(111) and 1.8 THz for Cs/Cu(111); these values are in consistence with the S mode frequencies found by other surface vibrational spectroscopy [10, 11]. Large oscillation amplitudes are observed only for coverages higher than $\theta \sim 0.6$. This is also the case for Cs/Pt(111) [7] and K/Pt(111) [26]: the S mode oscillation amplitudes in TRSHG signals are not proportional to the alkali coverage but show an onset at around a half monolayer. According to the discussion on the electronic structure of alkali overlayer, the formation of OR and QWS is the expected feature occurring at around half monolayer. Consequently, the coherent excitation of the S mode is in line with the emergence of these surface states.

6. Excitation Mechanisms for Na and K Overlayers on Cu(111)

The pump pulse creates hot electrons and holes in substrate and in the surface bands. However, not all electronic excitations are effective to couple with motions of alkali atoms. There are two extreme cases in photo-induced nuclear dynamics at surfaces, as has been frequently discussed in the studies of surface photochemistry: adsorbate-localized excitation versus substrate-mediated excitation. [27] For the alkali adsorption systems in the coverage range from $\theta = 0.5$ to 1.0, transitions of OR → QWS, OR → IPSs, and QWS → IPSs are candidates for the adsorbate-localized excitation. Intra- and interband excitations of s, p, and d bands of bulk are involved in the substrate-mediated excitation: electrons or holes created by the electronic excitation of bulk bands transiently transfer to the alkali-induced electronic state, resulting in modulation of the electron density near alkali adatoms. In addition, another possible excitation mechanism specific to alkali overlayers is the multipole plasmon excitation. This excitation produces a longitudinally oscillating electron density at an alkali-covered surface, which may also initiate the coherent motion of alkali adsorbates.

In order to distinguish the excitation mechanisms, the excitation photon energy dependence of the initial amplitude of the S mode coherent motion was measured for K/Cu(111) (Figure 4) [10]. The excitation photon energy dependence was found to resemble the absorption curve of bulk copper:

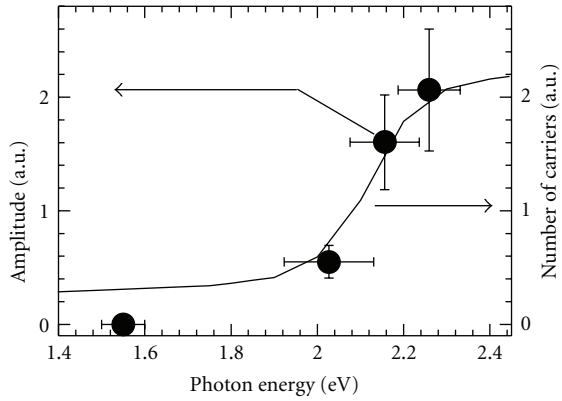

FIGURE 4: Excitation photon energy dependence of the initial amplitude of the coherent vibration of the S mode of K/Cu(111) (filled circles). The potassium coverage was 0.63 ML. Numerical estimation of the number of photogenerated carriers within the Cu substrate [10] (solid curve).

that corresponds well to the carrier density curve (solid curve) estimated from substrate absorption. Therefore, the substrate electronic excitation is likely responsible for the coherent phonon excitation of alkalis on copper. Similar results have been obtained also for Na/Cu(111) [9].

Because the emergence of oscillatory modulations in TRSHG traces is concomitant with stabilization of the QWS band to the Fermi level, it is likely that the population change in the QWS band is responsible for a driving force to alkali atoms along the alkali atom-Cu coordinate. One possible excitation path for generating the impulsive force is hole creation in the QWS. Electron-hole pairs are formed in the substrate by the d-band$\rightarrow s$, p-band transition, followed by subsequent Auger recombination of an electron in the QWS band with the d-band hole, resulting in creation of holes in the QWS. An appreciable coupling between the hole creation at the alkali-derived QWS and surface (or interface) phonon excitation has been suggested [28]. Alternatively, hot electrons created by the d-band$\rightarrow s$, p-band transition could be injected into the QWS above E_F, resulting in abrupt fluctuations of electron density at alkali atoms. In either case, the rapid changes in charge density at the surface, particularly in the QWS band, are likely to be the origin for the driving force along the alkali atom-Cu stretching coordinate.

7. Switching of the Excitation Mechanism for Cs/Cu(111) Depending on the Pump Photon Energy [11]

As has been described in the previous section, investigation on Na/Cu(111) and K/Cu(111) system has revealed that the S mode excitation occurs via substrate-mediated process. However, this is not the whole story, and here we show that the Cs monolayer on Cu(111) provides a good opportunity to elucidate further the excitation mechanisms [11]. A peculiar feature of the Cs/Cu(111) is that at high coverages, in addition to the OR and QWS bands, an unoccupied band originating from Cs 5d band is located at 1.6 eV above the Fermi level [29]. Thus, the resonance transition from QWS to the unoccupied Cs 5d band is expected to take place at around 1.6 eV. Note that no transitions take place from bulk Cu d bands at $h\nu = 1.6$ eV because the top of the Cu d bands are located at $\sim$2.0 eV below the Fermi level. Consequently, it is possible to examine how the characteristics of surface coherent phonons depend on the nature of electronic excitation by varying the excitation photon energy: adsorbate-localized excitation versus substrate-mediated excitation.

Figure 5(a) shows typical traces of TRSHG signals from Cs-covered Cu(111) ($\theta = 1$) for excitations at the wavelengths $\lambda_{ex} = 400$ and 800 nm. Although both TRSHG traces at $\lambda_{ex} = 800$ and 400 nm show a prominent oscillating component with frequency of 1.8 THz, the initial phase of the oscillating component at $\lambda_{ex} = 800$ nm is very different from that at $\lambda_{ex} = 400$ nm, as shown in Figure 5(b). Cs–Cu stretching is sin-like ($\phi = -81 \sim -103^\circ$) at $\lambda_{ex} = 800$ nm, while this is close to cos-like ($\phi = -144 \sim -161^\circ$) at $\lambda_{ex} = 400$ nm. The initial phase difference provides useful information of the temporal profiles of the driving force: it is impulsive like for $\lambda_{ex} = 800$ nm, but step function like for $\lambda_{ex} = 400$ nm (see (3)). In addition to the initial phase, the pump fluence dependence of the oscillation amplitude was found to be very different between $\lambda_{ex} = 400$ and 800 nm (Figure 6). While the amplitude at $\lambda_{ex} = 400$ nm increases linearly with the pump fluence, the amplitude at $\lambda_{ex} = 800$ nm shows strong saturation feature. This indicates that surface localized excitation plays a role at $\lambda_{ex} = 800$ nm.

8. Theoretical Modeling of the ExcitationMechanism [11]

The significant dependences on excitation photon energy found for Cs/Cu(111) indicate different excitation mechanisms operating for the two excitation photon energies. Since adsorbate-localized excitation is expected at $\lambda_{ex} = 800$ nm, Yasuike and Nobusada (YN) developed a theoretical modeling to rationalize the observed feature applying the transient-adsorbate mediation (TAM) mechanism recently proposed by themselves [30, 31].

The TAM mechanism is schematically depicted in Figure 7. Three potential energy curves (PECs) are considered: one is that of the ground state, $V_g(Z)$, and another one is that of the excited state with adsorbate localized nature, $V_e(Z)$, and the third one is that of bulk excited state, $V_b^\epsilon(Z)$. In the adsorbate-localized excited state, the Cs–Cu equilibrium distance is shifted from that in the ground state. In addition, the state has a finite width Γ because of interactions with bulk continuum electronic states. The bulk excited states are composed of a continuum caused by electron-hole pair creations in bulk bands. Unless bulk excitations lead to electron transfer to the adsorbate-localized unoccupied band, they do not directly trigger Cs nuclear motions. Thus, the potential energy curves of the bulk excited states $V_b^\epsilon(Z)$ are assumed to have the same Z dependence as $V_g(Z)$ but shifted vertically by the excitation energy of bulk electrons.

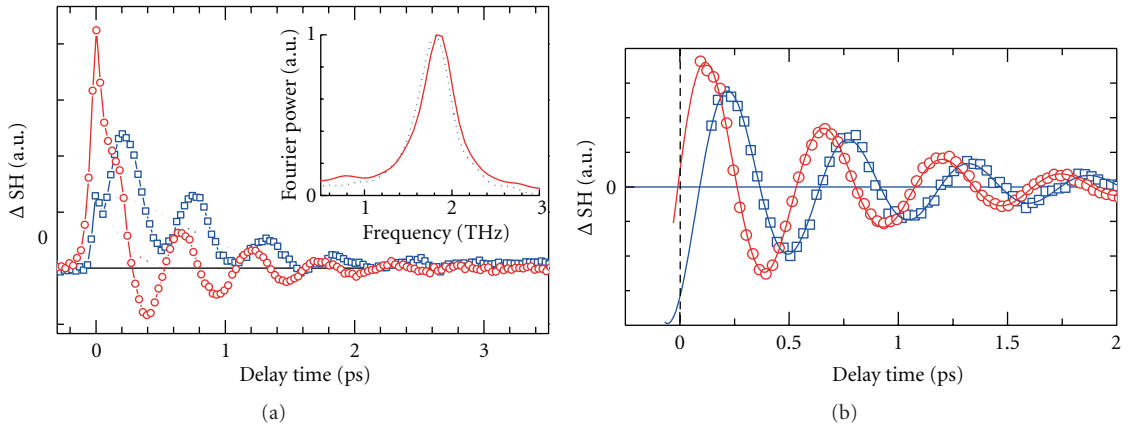

FIGURE 5: (a) TRSHG traces for Cs/Cu(111) with λ_{ex} = 800 nm (1.55 eV) (red) and 400 nm (3.10 eV) (blue). The probe wavelength was 565 nm (2.20 eV). Cs coverage was 0.8 ML for λ_{ex} = 800 nm and 0.9 ML for λ_{ex} = 400 nm. The inset shows the Fourier spectra of the oscillatory components. (b) The oscillatory parts of the TRSHG traces in (a). Reprinted with permission from [11]. Copyright (2011) American Chemical Society.

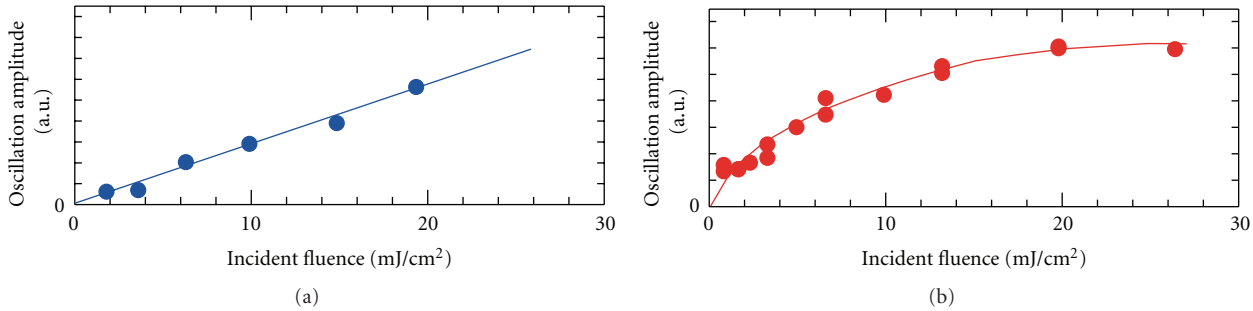

FIGURE 6: Incident pump fluence dependence of the initial amplitude of oscillation in TRSHG traces from Cs-covered Cu(111). The excitation wavelengths were (a) λ_{ex} = 400 nm nm (blue) and (b) λ_{ex} = 800 nm (red). Solid lines are guides to the eye. Reprinted with permission from [11]. Copyright (2011) American Chemical Society.

After the irradiation of near-resonant light pulse, the population partially transfers to the adsorbate-localized excited state. The wavepacket on this PEC starts to propagate toward vacuum owing to the repulsive force and gains momentum. Because the back donation of charge to the bulk occurs rapidly, the lifetime of this state is very short. Thus, the quenching of the adsorbate-localized excited state brings the wavepacket to the PEC of bulk continuum states; then, an oscillatory motion of the wavepacket takes place on the PEC, while bulk electrons dissipate energy via electron-phonon coupling.

From a numerical analysis based on the model, the sin-like initial phase and the saturation behavior in the pump fluence dependence were successfully reproduced [11]. Figure 8 shows initial phases calculated from TAM model as a function of the lifetime of the excited state. The sin-like behavior is due to a short lifetime in the adsorbate-localized state, and the saturation (Figure 6) originates primarily in the limited density of states of the initial state: only a small fraction of the QWS band is occupied.

At λ_{ex} = 400 nm, bulk excitations from the *d* bands of copper generate the coherent Cs–Cu stretching vibration. In contrast to the case of λ_{ex} = 800 nm, the coherent oscillation is nearly cos-like and the amplitude of oscillatory signals linearly increases with pump fluence (Figure 6). In general, absorption of an intense fs laser pulse generates quasithermal equilibrium in the surface electron gas, and its peak temperature reaches several thousand K over a time scale of several hundred fs. At λ_{ex} = 400 nm, the effect of the hot electrons may play a crucial role: under the circumstances, the adsorbate-localized state is temporarily occupied with hot electrons. The force exerted on Cs is generated by transient occupation of the adsorbate-localized band by resonant electron transfer from bulk bands. Because the excitation takes place much faster than the period of Cs–Cu stretching, the indirect excitation can coherently excite this mode. Note that the electron temperature decays with a slower time scale than the Cs–Cu oscillation period, and the driving force is no longer close to a delta function but rather like a step function.

YN proposed that the effective PEC for the adsorbate vibration excitation under the influence of the substrate hot electrons is given by [11, 32]

$$V_{\text{eff}}(Z) = V_g(Z) - \int_{-\infty}^{\infty} n_F(E, T_e)\delta(E, Z)dE, \qquad (9)$$

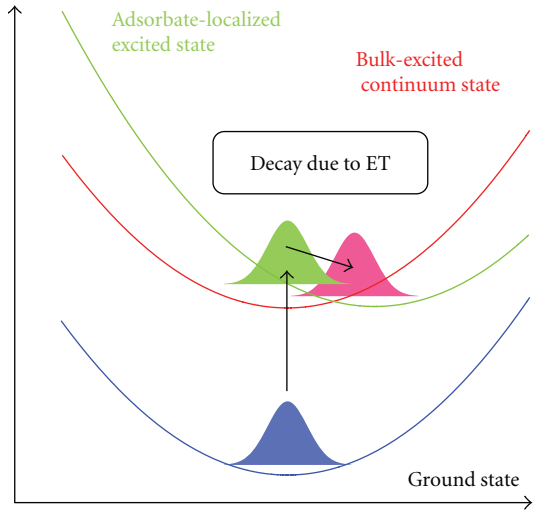

Figure 7: Schematic representation of the potential energy curves (PECs) of the TAM model: ground state (blue), the adsorbate-localized excited state (green), and the bulk continuum states (red). Reprinted with permission from [11]. Copyright (2011) American Chemical Society.

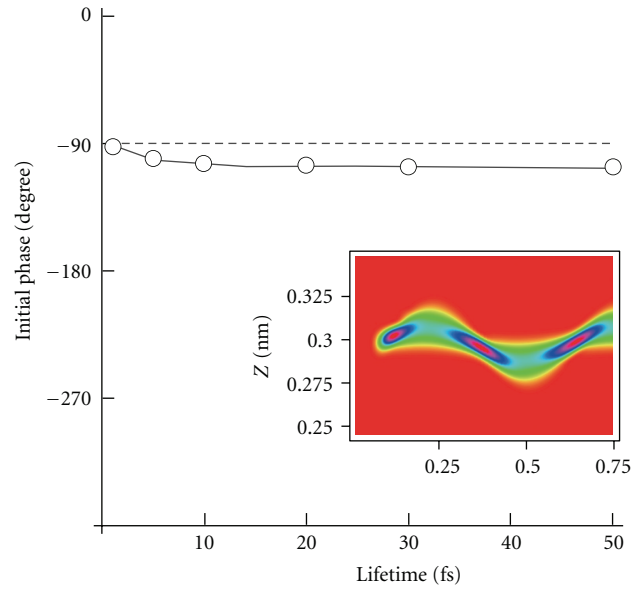

Figure 8: Initial phases calculated from TAM model as a function of the lifetime of the excited state. Inset: the time evolution of the wave packet. Reprinted with permission from [11]. Copyright (2011) American Chemical Society.

where $n_F(E, T_e)$ is the Fermi-Dirac distribution at electron temperature T_e. The function $\delta(E, Z)$ is an effective occupation number of the adsorbate-localized excited states and is defined by the integration of the local density of states for the adsorbate-localized excited state,

$$\delta(E, Z) = \frac{1}{\pi} \int_{-\infty}^{E} dE' \frac{\Gamma/2}{(E' - E_r)^2 + (\Gamma/2)^2}, \qquad (10)$$

where $E_r = \mathrm{Re}[V_e(Z)]$ and Γ is the effective band width. In the limit of the step function profile of the driving force, the oscillation should be pure cosine because Cs atoms oscillate on the displaced potential energy surface. However, we found experimentally that the oscillation deviates from the pure cosine function. Theoretical simulations using (9) and (10) successfully reproduced the deviations of initial phase from pure cosine by considering relaxation of hot electrons: the effective PEC shows a transient shift in line with the electron temperature decay, and the phase of the Cs vibration is modulated by the change of the PEC. In addition, the simulations verify the linear dependence of the initial amplitude on the pump fluence if the band width of the unoccupied state is 1.0 eV [11].

9. Summary and Outlook

We describe the principle of time-resolved SHG spectroscopy under an ultrahigh vacuum condition and its application to the alkali metal adsorption systems. Electronic excitation of the adsorption systems by ultrafast laser pulses induces coherent surface phonons. The large enhancement in SH intensity at the alkali-covered metal surfaces allows to monitor precisely the time-evolution of the coherent phonons. Electronic excitations of both adsorbate-induced and substrate bands by using ultrafast light pulses can induce abrupt fluctuations of charge density around alkali adatoms, resulting in coherent nuclear motions of adsorbates via electron-phonon couplings. For Na and K/Cu(111), excitation-photon-energy dependence for coherent surface phonons clearly indicates that substrate electronic excitation induces the coherent motions of the S mode. For Cs/Cu(111), we observed clear switching of the excitation mechanism from bulk excitation for $\lambda_{ex} = 400$ nm to adsorbate localized excitation at $\lambda_{ex} = 800$ nm. Attempts for theoretical modeling of the both excitation processes have been described.

TRSHG is versatile to investigate coherent phonon dynamics at surfaces. This method is ideally suited for alkali overlayers because of the marked enhancement of SH intensity. However, applications of TRSHG to other adsorption systems have been very limited, mainly because they lack such large enhancement in SH intensity. This obstacle can be removed if SH intensity is enhanced by tuning the photon energy of probe pulses to an electronic resonance of adsorption systems. In addition, using much shorter pump pulses extends the applicability of TRSHG to coherent surface phonons and adsorbate vibrations at higher frequencies.

Acknowledgments

The authors would like to thank their collaborators in the research program summarized in this paper. This work was supported in part by Grants-in-Aid for Scientific Research (S) (Grant no. 17105001) and for Young Scientists (B) (Grant no. 19750012) from Japan Society for the Promotion of Science (JSPS) and Scientific Research on Priority Area (461 Molecular Theory for Real Systems) from the Ministry of

Education, Culture, Sports, Science and Technology (MEXT) of Japan. K. Watanabe gratefully acknowledges financial support by the PRESTO program of JST.

References

[1] L. Dhar, J. A. Rogers, and K. A. Nelson, "Time-resolved vibrational spectroscopy in the impulsive limit," *Chemical Reviews*, vol. 94, no. 1, pp. 157–193, 1994.

[2] T. Dekorsy, G. C. Cho, and H. Kurz, "Coherent phonons in condensed media," in *Topics in Applied Physics*, vol. 76, chapter 4, pp. 169–209, Springer, Berlin, Germany, 2000.

[3] D. M. Riffe and A. J. Sabbah, "Coherent excitation of the optic phonon in Si: transiently stimulated Raman scattering with a finite-lifetime electronic excitation," *Physical Review B*, vol. 76, no. 8, Article ID 085207, 2007.

[4] Y. M. Chang, L. Xu, and H. W. K. Tom, "Observation of coherent surface optical phonon oscillations by time-resolved surface second-harmonic generation," *Physical Review Letters*, vol. 78, no. 24, pp. 4649–4652, 1997.

[5] K. Watanabe, N. Takagi, and Y. Matsumoto, "Impulsive excitation of a vibrational mode of Cs on Pt (1 1 1)," *Chemical Physics Letters*, vol. 366, no. 5-6, pp. 606–610, 2002.

[6] K. Watanabe, N. Takagi, and Y. Matsumoto, "Direct time-domain observation of ultrafast dephasing in adsorbate-substrate vibration under the influence of a hot electron bath: Cs adatoms on Pt(111)," *Physical Review Letters*, vol. 92, no. 5, pp. 574011–574014, 2004.

[7] K. Watanabe, N. Takagi, and Y. Matsumoto, "Femtosecond wavepacket dynamics of Cs adsorbates on Pt(111): coverage and temperature dependences," *Physical Review B*, vol. 71, no. 8, Article ID 085414, 9 pages, 2005.

[8] Y. Matsumoto and K. Watanabe, "Coherent vibrations of adsorbates induced by femtosecond laser excitation," *Chemical Reviews*, vol. 106, no. 10, pp. 4234–4260, 2006.

[9] M. Fuyuki, K. Watanabe, D. Ino, H. Petek, and Y. Matsumoto, "Electron-phonon coupling at an atomically defined interface: Na quantum well on Cu(111)," *Physical Review B*, vol. 76, no. 11, Article ID 115427, 2007.

[10] K. Watanabe, K. I. Inoue, I. F. Nakai, M. Fuyuki, and Y. Matsumoto, "Ultrafast electron and lattice dynamics at potassium-covered Cu(111) surfaces," *Physical Review B*, vol. 80, no. 7, Article ID 075404, 2009.

[11] K. Watanabe, Y. Matsumoto, T. Yasuike, and K. Nobusada, "Adsorbate-localized versus substrate-mediated excitation mechanisms for generation of coherent Cs-Cu stretching vibration at Cu(111)," *Journal of Physical Chemistry A*, vol. 115, no. 34, pp. 9528–9535, 2011.

[12] R. D. Diehl and R. McGrath, "Structural studies of alkali metal adsorption and coadsorption on metal surfaces," *Surface Science Reports*, vol. 23, no. 2-5, pp. 43–171, 1996.

[13] S. E. Finberg, J. V. Lakin, and R. D. Diehl, "He-atom scattering study of the vibrational modes of alkalis on Al(111)," *Surface Science*, vol. 496, no. 1-2, pp. 10–20, 2002.

[14] A. P. Graham, "The low energy dynamics of adsorbates on metal surfaces investigated with helium atom scattering," *Surface Science Reports*, vol. 49, no. 4-5, pp. 115–168, 2003.

[15] S. Lindgren and L. Walldén, "Some properties of metal overlayers on metal substrates," in *Handbook of Surface Science*, vol. 2, chapter 13, pp. 899–951, Elsevier, Amsterdam, The Netherlands, 2000.

[16] A. Liebsch, *Electronic Excitations at Metal Surfaces. Physics of Solids and Liquids*, Plenum Press, New York, NY, USA, 1997.

[17] J. P. Gauyacq, A. G. Borisov, and M. Bauer, "Excited states in the alkali/noble metal surface systems: a model system for the study of charge transfer dynamics at surfaces," *Progress in Surface Science*, vol. 82, no. 4–6, pp. 244–292, 2007.

[18] R. W. Gurney, "Theory of electrical double layers in adsorbed films," *Physical Review*, vol. 47, no. 6, pp. 479–482, 1935.

[19] E. Wimmer, "All-electron local density functional study of metallic monolayers. I. Alkali metals," *Journal of Physics F*, vol. 13, no. 11, article no. 014, pp. 2313–2321, 1983.

[20] H. W. K. Tom, C. M. Mate, X. D. Zhu, J. E. Crowell, Y. R. Shen, and G. A. Somorjai, "Studies of alkali adsorption on Rh(111) using optical second-harmonic generation," *Surface Science*, vol. 172, no. 2, pp. 466–476, 1986.

[21] Y. R. Shen, "Wave mixing spectroscopy for surface studies," *Solid State Communications*, vol. 102, no. 2-3, pp. 221–229, 1997.

[22] A. Liebsch, "Second-harmonic generation from alkali-metal overlayers," *Physical Review B*, vol. 40, no. 5, pp. 3421–3424, 1989.

[23] J. Zhao, N. Pontius, A. Winkelmann et al., "Electronic potential of a chemisorption interface," *Physical Review B*, vol. 78, no. 8, Article ID 085419, 7 pages, 2008.

[24] P. J. Feibelman, "Surface electromagnetic fields," *Progress in Surface Science*, vol. 12, no. 4, pp. 287–407, 1982.

[25] Y. M. Chang, L. Xu, and H. W. K. Tom, "Coherent phonon spectroscopy of GaAs surfaces using time-resolved second-harmonic generation," *Chemical Physics*, vol. 251, no. 1–3, pp. 283–308, 2000.

[26] M. Fuyuki, K. Watanabe, and Y. Matsumoto, "Coherent surface phonon dynamics at K-covered Pt(111) surfaces investigated by time-resolved second harmonic generation," *Physical Review B*, vol. 74, no. 19, Article ID 195412, 2006.

[27] W. Ho, "Surface photochemistry," in *Laser Spectroscopy and Photochemistry on Metal Surfaces Part II*, chapter 24, pp. 1047–1140, World Scientific Publishing, River Edge, NJ, USA, 1995.

[28] E. V. Chulkov, J. Kliewer, R. Berndt et al., "Hole dynamics in a quantum-well state at Na/Cu(111)," *Physical Review B*, vol. 68, no. 19, Article ID 195422, 2003.

[29] D. A. Arena, F. G. Curti, and R. A. Bartynski, "Unoccupied electronic states of the Cs/Cu(100) and Cs/Cu(111) adsorption systems," *Physical Review B*, vol. 56, no. 23, pp. 15404–15411, 1997.

[30] T. Yasuike and K. Nobusada, "Open-boundary cluster model for calculation of adsorbate-surface electronic states," *Physical Review B*, vol. 76, no. 23, Article ID 235401, 2007.

[31] K. Nobusada and T. Yasuike, "Photoinduced coherent adsorbate dynamics on a metal surface: nuclear wave-packet simulation with quasi-diabatic potential energy curves using an open-boundary cluster model approach," *Physical Review B*, vol. 80, no. 3, Article ID 035430, 2009.

[32] M. Brandbyge, P. Hedegård, T. F. Heinz, J. A. Misewich, and D. M. Newns, "Electronically driven adsorbate excitation mechanism in femtosecond-pulse laser desorption," *Physical Review B*, vol. 52, no. 8, pp. 6042–6056, 1995.